Journal of Photochemistry and Photobiology A: Chemistry 198 (2008) 288–292

Contents lists available at ScienceDirect

Journal of Photochemistry and Photobiology A: Chemistry

journal homepage: www.elsevier.com/locate/jphotochem

Poly(*o*-phenylenediamine)/MWNTs composite film as a hole conductor in solid-state dye-sensitized solar cells

Xiu-Hua Zhang, Shi-Min Wang*, Zu-Xun Xu, Jie Wu, Lin Xin

Ministry-of-Education Key Laboratory for the Synthesis and Application of Organic Functional Molecules, Hubei University, Wuhan 430062, People's Republic of China

ARTICLE INFO

Article history:
Received 24 October 2007
Received in revised form 26 February 2008
Accepted 8 April 2008
Available online 16 April 2008

Keywords:
Dye-sensitized solar cells
Poly(*o*-phenylenediamine)/MWNTs
Composite film
Electrochemical polymerization

ABSTRACT

All solid-state dye-sensitized solar cells were fabricated using in situ electrochemically polymerized poly(*o*-phenylenediamine)/MWNTs (PoPD/MWNTs) as a hole transport materiel. The electrochemical behaviors of PoPD/MWNTs indicated that the electron exchange efficiency improves obviously of PoPD after the addition of carbon nanotubes. The PoPD/MWNTs composite film was deposited on the dye anchored porous TiO_2 electrode and *I–V* characterization was performed under simulated AM 1.5 illumination. Fabricated devices for the PoPD/MWNT composites prepared in 0.1 g/L MWNTs showed a photoresponse with an open-circuit voltage V_{OC} of 479 mV and a short-circuit current density (I_{SC}) of 0.572 mA/cm^2 with the overall conversion efficiency of 0.13%, higher than those of the cell with only PoPD (i.e., I_{SC} = 0.275 mA/cm^2, V_{OC} = 462 mV, FF = 0.35, η = 0.04%). It is obvious that the introduction of MWNTs to PoPD composites could improve the cell performance.

1. Introduction

Since the first description in the beginning of the 1990s by O'Regan and Grätzel [1], dye-sensitized solar cells (DSSC) based on nanocrystalline inorganic oxides such as TiO_2, ZnO and SnO_2 have attracted much attention because of its lower cost and potential alternatives to traditional photovoltaic device [2,3]. The overall efficiency of this new type of solar cell based on liquid electrolytes using organic compound, such as acetonitrile, propylene carbonate and ethylene carbonate as solvent and iodide/triiodide (I^-/I^{3-}) redox couple as electrolyte have reached 10–11% under irradiation of AM 1.5 [4,5], which is comparable to that of amorphous silicon solar cells [6]. However, this type of liquid-junction cell remains some problems, which limit their practical applications [6,7]. Therefore, there is considerable interest in the development of solid-state electrolyte for such devices [8]. At present, many research groups have been searching for alternatives to replace the liquid electrolytes, such as inorganic p-type semiconductors [9], ionic liquids [10–12], polymeric/inorganic nanocomposites containing I^-/I_3^- redox couple [13,14] or organic hole transport materials (HTMs) [8,15,16].

Carbon nanotubes (CNTs) have received significant interest because of their dimensions and structure-sensitive properties since CNTs were discovered by Iijima in 1991 [17]. CNTs show electrical properties as metal or semiconductors, depending on their size and lattice helicity [18]. The subtle electronic properties suggest that CNTs, when used as an electrode material in electrochemical reactions, have the ability to promote electron-transfer reactions, which represents a new application of carbon nanotubes [19,20]. Incorporation of CNTs into conducting polymers can lead to new composite materials possessing the properties of each component with a synergistic effect that would be useful in particular applications [21,22], which lead nanotubes became the ideal additives for structural and functional composites. For example, epoxy resin added only 1% SWNTs showed a 70% increase in thermal conductivity at 40 K, increasing to 125% at room temperature [23] and the introduction of MWNTs to polyaniline composites would enhance the electrical properties by facilitating charge-transfer processes between the two components [24].

The feasibility of incorporating SWNTs into a conducting polymer for photovoltaic devices has been reported by Kymakis and co-workers in 2002. Their results showed a diode response for devices constructed in the sandwich formation, containing the arc-generated SWNT-poly-(3-octylthiophene) composite film between an indiumtin-oxide (ITO) front contact and aluminum back contact. There was a photoresponse under AM 1.5 illumination for both the pristine P3OT device and a 1% SWNT-P3OT composite blend, albeit the composite exhibits current densities several orders of magnitude higher [25]. Raffaelle and co-workers has also reported a photovoltaic device containing 1% (w/w) SWNTs in P3OT. This device has shown a photoresponse with low current densities, but relatively high open-circuit voltages (~1 V) [26].

* Corresponding author. Tel.: +86 27 88662747.
E-mail address: wangsm.hubu@yahoo.com.cn (S.-M. Wang).

1010-6030/$ – see front matter © 2008 Elsevier B.V. All rights reserved.
doi:10.1016/j.jphotochem.2008.04.006

In this paper, we report the fabrication of solid-state DSSC using in situ electrochemically polymerized poly(*o*-phenylenediamine)/MWNTs composite film as a hole transport phase. The in situ electrochemically polymerization of PoPD/MWNTS in the mesoporous electrodes could make a good contact between the dye molecules and hole transport material. In addition, introduction of MWNTs to PoPD composites would enhance the electrical properties by facilitating charge-transfer processes, which would improve the cell performance.

2. Experimental

2.1. Materials

o-Phenylenediamine (oPD) ~99% (Aldrich Chemical Co.) was sublimated under vacuum at 80 °C before use. Other reagents were used without further purification. MWNTs, synthesized by AC carbon arc discharge method (Wuhan University, China) were treated with acid in an ultrasonication bath prior to use to ensure a high dispersion quality. Specifically, to eliminate impurities in the MWNT (such as metallic catalysts), they were treated with 3 M HNO_3 at 60 °C for 12 h which produced carboxylic acid (—COOH) functional groups at the defect sites.

2.2. Preparation of nanoparticulate TiO_2 film and adsorption of dye

The DSSC (with the active area of 0.125 cm^2) were constructed according to the following procedure. Transparent glasses coated with a conductive indium tin oxide (ITO, sheet resistance 8 Ω/cm^2, made by Beijing Building Material Factory, China) were used for the photo-electrode and counter-electrode. For fabrication of the photo-electrode, a compact TiO_2 layer was firstly deposited on an optically transparent conducting glass as reported by Refs. [27,28] to avoid a direct contact between the HTMs and the ITO, which causes short circuit of the cell. A commercial mesoporous TiO_2 paste was deposited using doctor blade onto the ITO glass and sintered for 30 min at 450 °C in oven (heating rate: 10 °C/min). Thickness of the TiO_2 was around 5 μm. When cooling to 80 °C, the TiO_2 electrode was immersed in a 5.0×10^{-4} M N719 dye (Solaronix Co.) in ethanol solution at room temperature for 24 h in the dark. The electrode was then rinsed with ethanol and dried.

2.3. Fabrication of a dye-sensitized TiO_2 cell

Electropolymerization of PoPD/MWNTs composite film onto the dye anchored porous TiO_2 electrode was carried out in a 0.1 M $HClO_4$ acetonitrile solution containing 0.05 M oPD and different concentration MWNTs (dissolving sonically for 10 min) by cyclic voltammetry with the potential scanning range of −0.3 to 1.0 V at 0.1 V s^{-1} scan rate for 50 cycles. A three-electrode system was used in the electropolymerization, with a dye-adsorbed TiO_2 on ITO as the working electrode, an Ag/AgCl as the reference electrode and a platinum wire as the auxiliary electrode. After polymerization, PoPD/MWNTs/dye/TiO_2 electrode was rinsed with ethanol and dried at room temperature. Electrical contact to the PoPD/MWNTs composite film surface is made by pressing a Pt-sputtered conducting glass plate onto it. The DSSC are clamped with two clips.

2.4. Measurements

Electrochemical experiments were carried out with PARSTAT 2263 electrochemical system (Princeton Applied Research, USA) controlled by a personal computer. The conductivities of PoPD and PoPD/MWNTs composites are measured using the standard Van Der Pauw DC four-probe method in the dark or under light (1 Sun, 100 mW/cm^2) at room temperature. The electrical conductivity of samples was calculated by the following formula: $\sigma(S/cm) = (2.44 \times 10/S) \times (I/E)$, where σ is the conductivity; S is the sample side area; I is the current passed through outer probes; E is the voltage drop across inner probes [29]. The I–V characteristics were measured with a Keithley 2400 source meter under dark or an illumination of AM 1.5 (1 Sun, 100 mW/cm^2) using a solar simulator (Model 91192-1000, Oriel instruments, USA). Transmission electron microscopic (TEM) images were obtained by using a JEOL JEM-100SX microscope (Japan). X-ray diffraction patterns (XRD) were obtained with a D/MAX-IIIc diffractometer (Japan).

3. Results and discussion

The morphology of the resulting PoPD and PoPD/MWNTs composite were characterized by TEM (Fig. 1). The TEM images clearly show that two different types of materials are visible. The diameter of the PoPD was about 50–80 nm (Fig. 1a). The individual fibrous phases of PoPD/MWNTs composite have diameters between 100 and 130 nm (Fig. 1b), and therefore must be the MWNTs (diameter 20–30 nm) coated with PoPD polymer layers. In addition, the PoPD/MWNTs composite displayed a special three-dimensional nanoporous structure which made it possible to form a large number of micropores. This indicates the nanoporous PoPD/MWNTs composite would have lager surface area that of PoPD and would enhance the electrical properties by facilitating charge-transfer processes.

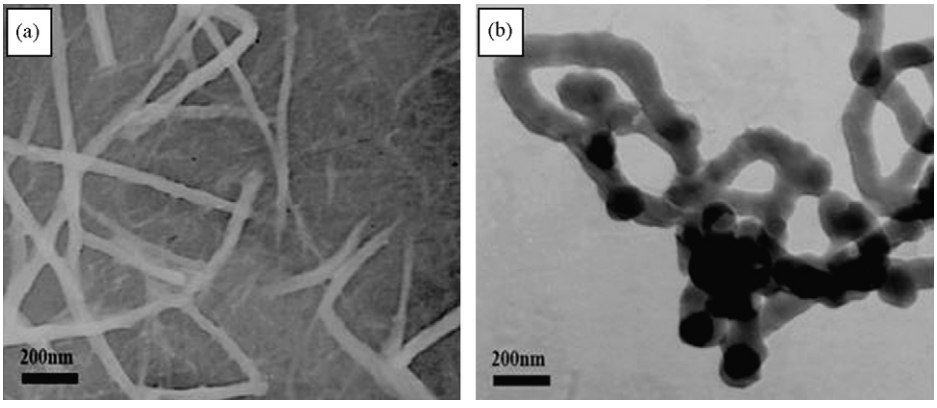

Fig. 1. TEM images of PoPD (a) and PoPD/MWNTs composite films (b) obtained by repeat cyclic voltammetric scanning.

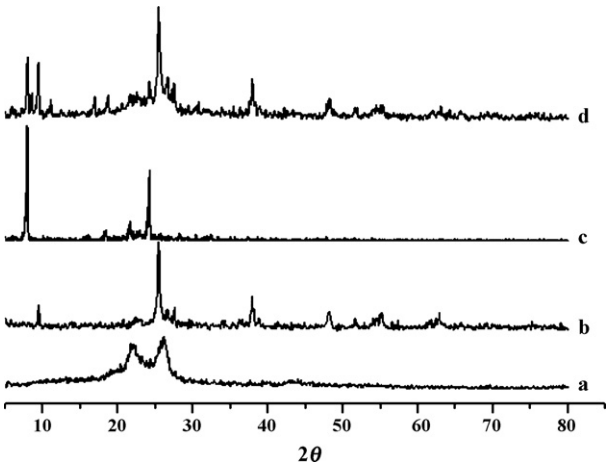

Fig. 2. XRD scattering patterns of MWNTs (a); dye/TiO_2 (b); PoPD (c) and PoPD/MWNTs/dye/TiO_2 (d).

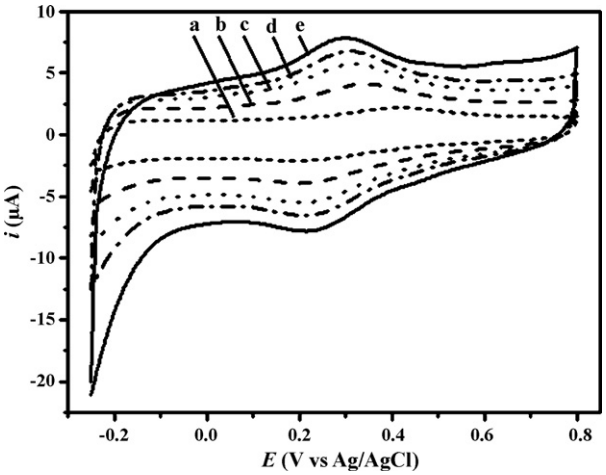

Fig. 3. Cyclic voltammograms of the PoPD (a) and the PoPD/MWNTs (b–e) deposited on ITO at different concentrations of MWNTs in 0.1 M $HClO_4$ acetonitrile solution. Scan rate: 50 mV s^{-1}. MWNTs concentration: (a) 0, (b) 0.02 g/L, (c) 0.05 g/L, (d) 0.1 g/L, (e) 0.15 g/L.

The mechanism for the formation of fibrous composite could be associated with the weak interaction between oPD monomer and MWNTs. The interaction possibly involves the π–π electron interaction between MWNTs and the oPD monomer, and the hydrogen bond interaction between the carboxyl groups of MWNTs and imino groups of oPD monomers. Such interaction ensures the adsorption of oPD monomer on the surface of MWNTs during the formation of fibrous phase composite. MWNTs therefore serve as the template and the core during the formation of the fibrous phase composites, which is similar to the formation of PANI/MWNT composites with tubular nanostructure [29,30].

Fig. 2 shows the X-ray diffraction patterns for MWNTs, dye/TiO_2 electrode, PoPD and PoPD/MWNTs/dye/TiO_2 electrode. For MWNT (a), the diffraction peaks were observed at $2\theta = 22.1^\circ$ and 26.1°, corresponding to a graphite-like structure. For dye/TiO_2, the crystalline peaks of 25.4°, 27.5° correspond to TiO_2. Meanwhile, for PoPD samples, crystalline peaks at 8.1° and 24.4° were observed, indicating that the PoPD samples have better crystallinity. The X-ray data of PoPD/MWNT/dye/TiO_2 reveal crystalline peaks similar to those obtained from the MWNT, PoPD and dye/TiO_2, indicating that no additional crystalline order had been introduced into the electrode. The results indicate the PoPD/MWNTs composite films have been electrodeposited on the surface of dye/TiO_2 electrode.

Fig. 3 shows the cyclic voltammograms of the PoPD (Fig. 2a) and the PoPD/MWNTs (Fig. 2b–e) deposited on ITO at different concentrations of MWNTs in 0.1 M $HClO_4$ acetonitrile solution. Two couples of redox peaks can be observed for both kinds of films. The background currents of PoPD/MWNTs were apparently larger than that of PoPD, which indicates that PoPD/MWNTs has larger effective surface area. In addition, the peak currents of PoPD/MWNTs are higher than that of PoPD. Since this peak is associated with the polymerization of oPD, it can be inferred that a larger amount of the polymer has been electrodeposited on the ITO electrode surface in the presence of carbon nanotubes. This phenomenon is due to the attachment of the MWNTs on the electrode surface which provides an extended specific surface area and culminates in strengthening the electrochemical process. Therefore, larger amounts of the electro-active film can be deposited on the substrate [31,32]. Another distinction can be concluded from the peak separations between the anodic and cathodic peak, ΔE_p, which were listed in Table 1. With the increment of MWNTs, the ΔE_p tend to decrease and do not change obviously when the MWNTs concentration exceeded 0.1 g/L. The ΔE_p is taken as an estimate of the reversibility of the redox reaction [33]. Values of 0.074, 0.078, 0.093 and 0.129 V are obtained for the redox reactions of PoPD with carbon nanotube incorporation. They are smaller than the corresponding ΔE_p values of 0.199 V for pure PoPD film. According to theory of Laviron, if the ΔE_p is less than 200 mV/n, the average electron-transfer rate constant (k_s) can be calculated using the following equation [34,35]:

$$k_s = \frac{mnvF}{RT} \quad (1)$$

where m is a constant which is relative to the ΔE_p and can be obtained from Ref. [35], n the number of electrons involved in oxidation–reduction process ($n = 1$ according to [36]). F, R, T and v have their usual significance. From the peak-to-peak separation at scan rate of 50 mV s^{-1}, the k_s was calculated and listed in Table 1.

The conductivities of PoPD and PoPD/MWNTs composites were measured in the dark and under light and shown in Fig. 4 The PoPD shows conductivity of 5.65×10^{-6} S/cm in the dark and 3.4×10^{-4} S/cm in light, respectively. The PoPD/MWNTs electropolymerized in the solution containing 0.02 g/L MWNTs, the conductivities of the composite dramatically increase to 6.29×10^{-6} S/cm in the dark and 5.5×10^{-3} S/cm in light. With the continuous increase in the concentration of MWNTs, the conductivities gradually increase. The conductivities of the composite did not increase markedly when the concentration of MWNTs exceeded 0.1 g/L. The greatly different conductivities of composites in the dark and under light would be due to photoconduction of the PoPD [37]. Both the results of electron-transfer rate constant (k_s) and the conductivities indicate that the introduction of MWNTs to polymer composites would enhance the electrical properties by facilitating charge-transfer processes. The MWNTs probably serve as a "conducting bridge" and a doping agent during the PoPD conducting domains, which increase the effective percolation [38]. The effect

Table 1
Data obtained from cyclic voltammograms

Sample	Potential			k_s (s^{-1})
	E_{on} (V)	E_{RD} (V)	ΔE_P (V)	
PoPD	0.407	0.208	0.199	0.15
PoPD/MWNTs (0.02 g/L)	0.342	0.213	0.129	0.32
PoPD/MWNTs (0.05 g/L)	0.311	0.218	0.093	0.56
PoPD/MWNTs (0.1 g/L)	0.299	0.221	0.078	0.69
PoPD/MWNTs (0.15 g/L)	0.297	0.223	0.074	0.72

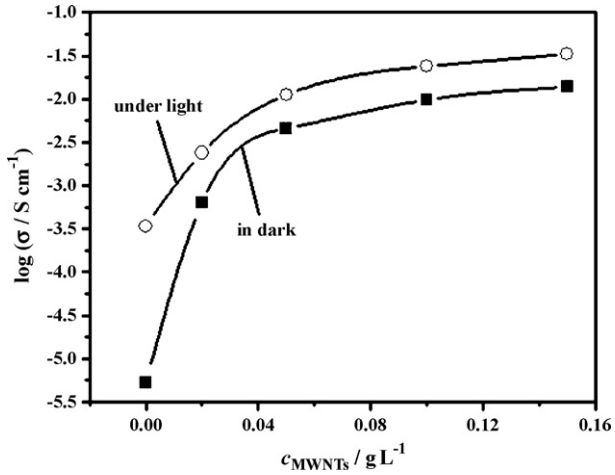

Fig. 4. Plot of the log of the conductivity of PoPD/MWNT composites with the concentration of MWNT in the dark and under light.

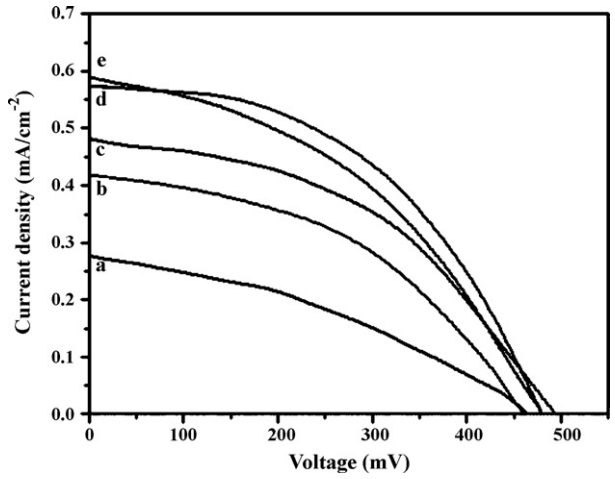

Fig. 5. *I–V* curves of the fabricated DSSC using PoPD (a) and PoPD/MWNTs (b–e) under an illumination of AM 1.5 condition.

of multi-wall nanotubes can also be related to increased roughness of the surface layer, which maybe improves electron exchange efficiency of PoPD. In addition, we consider the polymer composite is photoconductive and it functions also as "glue" that binds nanotube together.

Fig. 5 displays the *I–V* curves of the DSSC with PoPD and PoPD/MWNTs films as HTMs under 100 mW/cm^2 illumination and Table 2 enlists other parameters of solar cells. The value of open-circuit voltage, V_{OC}, does not obviously change with subsequent increase in PoPD/MWNTs from 0 to 0.15 g/L. However, for PoPD/MWNTs, value of short-circuit photocurrent density (I_{SC}) is found to be increased markedly from 0.275 to 0.591 mA/cm^2, when compared to cell prepared with PoPD as HTM. With increase in MWNTs concentration, the gradual increase in I_{SC}, is attributed to

Table 2
Cell performances of the solid-state dye-sensitized solar cells

HTMs	V_{OC} (mV)	I_{SC} (mA/cm^2)	FF (%)	Efficiency (%)
PoPD	462	0.275	35	0.04
PoPD/MWNTs (0.02 g/L)	457	0.415	44	0.08
PoPD/MWNTs (0.05 g/L)	491	0.479	44	0.1
PoPD/MWNTs (0.1 g/L)	479	0.572	49	0.13
PoPD/MWNTs (0.15 g/L)	478	0.591	42	0.12

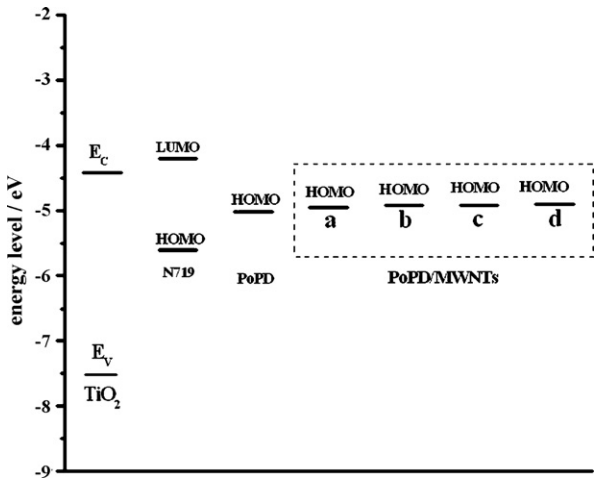

Fig. 6. Overview of the energy levels of the measured materials. The HOMO of the PoPD and PoPD/MWNTs were estimated from the onset of oxidation from Fig. 3 The valence band (VB) and conduction band (CB) of TiO_2 are indicated [39], as well as the HOMO and LUMO of N719. MWNTs concentration: (a) 0.02 g/L, (b) 0.05 g/L, (c) 0.1 g/L, (d) 0.15 g/L.

the increase the electron exchange efficiency of PoPD in DSSC. However, subsequent increase in concentration of MWNTs (from 0.1 to 0.15 g/L) does not help to increase the value of conversion efficiency further.

An energy band diagram, Fig. 6, has been constructed based on data gathered from Fig. 3 to illustrate the relative energetics of the polymer to the TiO_2 and N719 in our cell system. From this figure, it can be seen that the HOMO levels of PoPD/MWNTs is slightly above that of PoPD. It seems that the performances of all cells should not be great difference, which did not match with the real results obtained above. It could be explained as follows: under light irradiation, the photo-excited electrons in the molecules were injected into the conduction band of TiO_2, and the higher conductivity of the PoPD/MWNTs composites played an important role in the regeneration of the oxidized dye sensitizers to get high photocurrent (I_{SC}) and in reduction of the ohmic contacts to get high fill factor (FF) for the solid-state DSSC [8].

4. Conclusions

The ability to construct solid-state DSSC with polymer/MWNTS composites film as a hole transport materiel has been demonstrated. Introduction of MWNTs to PoPD composites enhance obviously the electrical properties by facilitating charge-transfer processes and improve the cell performance. Because many parameters of the cell assembly have not yet been optimized, further improvement of the photovoltaic performance is expected and underway. In particular, future work will focus on in detail characterizing the PoPD/MWNTs morphology inside the TiO_2 nanopores and inhibiting interfacial charge recombination.

Acknowledgement

This work was supported by the Chinese National Natural Science Foundation (2047201), the Key Laboratory Foundation for the Polymer Material and the Foundation for Outstanding Scholarship of Hubei Province.

References

[1] B. O'Regan, M. Grätzel, Nature 353 (1991) 737–740.

[2] M.K. Nazeeruddin, A. Kay, I. Rodicio, M. Grätzel, J. Am. Chem. Soc. 115 (1993) 6382–6385.
[3] M.K. Nazeeruddin, P. Pechy, M. Grätzel, J. Am. Chem. Soc. 123 (2001) 1613–1615.
[4] C.J. Barbe, F. Arendse, P. Comte, M. Grätzel, J. Am. Chem. Soc. 80 (1997) 3157–3160.
[5] M. Grätzel, J. Photochem. Photobiol. A: Chem. 164 (2004) 3–14.
[6] B. Li, L.D. Wang, B.N. Kang, P. Wang, Y. Qiu, Sol. Energy Mater. Sol. Cells 90 (2006) 549–573.
[7] M. Matsumoto, Y. Wada, T. Kitamura, K. Shigaki, T. Inoue, M. Ikeda, S. Yanagida, Bull. Chem. Soc. Jpn. 74 (2001) 387–390.
[8] C.N. Zhang, K.J. Wang, L.H. Hu, F.T. Kong, L. Guo, J. Photochem. Photobiol. A: Chem. 189 (2007) 329–333.
[9] K. Tennakone, G.R.R.A. Kumara, I.R.M. Kottegoda, K.G.U. Wijayantha, V.P.S. Perera, J. Phys. D: Appl. Phys. 31 (1998) 1492–1495.
[10] P. Wang, S.M. Zakeeruddin, R. Humphry-Baker, M. Grätzel, Mater. Chem. 16 (2004) 2694–2696.
[11] W. Kubo, T. Kitamura, K. Hanabusa, Y. Wada, S. Yanagida, Chem. Commun. (2002) 374–375.
[12] P. Wang, S.M. Zakeeruddin, P. Comte, I. Exnar, M. Grätzel, J. Am. Chem. Soc. 125 (2003) 1166–1167.
[13] A.F. Nogueira, J.R. Durrant, M.-A. De Paoli, Adv. Mater. 13 (2001) 826–829.
[14] T. Stergiopoulos, I.M. Arabatzis, G. Katsaros, P. Falaras, Nanoletters 2 (2002) 1259–1261.
[15] U. Bach, D. Lupo, P. Comte, J.E. Moser, F. Weissörtel, J. Salbeck, H. Spreitzer, M. Grätzel, Nature 395 (1998) 583–586.
[16] D. Gebeyehu, C.J. Brabec, N.S. Sariciftci, D. Vangeneugden, R. Kiebooms, D. Vanderzande, F. Kienbeerger, H. Schindler, Synth. Met. 125 (2002) 279–281.
[17] S. Iijima, Nature (London) 354 (1991) 56–58.
[18] P.J. Britto, K.S.V. Santhanam, P.M. Ajayan, Bioelectrochem. Bioenerg. 41 (1996) 121–125.
[19] F. Valentini, S. Orlanducci, M.L. Terranova, A. Aminec, G. Palleschi, Sens. Actuators B 100 (2004) 117–125.
[20] P.F. Liu, J.H. Hu, Sens. Actuators B 84 (2002) 94–199.
[21] M.L. Guo, J.H. Chen, J. Li, B. Tao, S.Z. Yao, Anal. Chim. Acta 532 (2005) 71–77.
[22] J.H. Kim, A.K. Sharma, Y.S. Lee, Mater. Lett. 60 (2006) 1697–1701.
[23] M.J. Biercuk, M.C. Llaguno, M. Radosavljevic, J.K. Hyun, A.T. Johnson, J.E. Fischer, Appl. Phys. Lett. 80 (2002) 2767–2769.
[24] M. Cochet, W.K. Maser, A.M. Benito, M.A. Callejas, M.T. Martinez, J.M. Benoit, Chem. Commun. 3 (2001) 1450–1451.
[25] E. Kymakis, G.A.J. Amaratunga, Appl. Phys. Lett. 80 (2002) 112–114.
[26] B.J. Landi, R.P. Raffaelle, S.L. Castro, BaileyF S.G., Prog. Photovolt: Res. Appl. 13 (2005) 165–172.
[27] Y. Saito, N. Fukuri, R. Senadeera, T. Kitamura, Y. Wada, S. Yanagida, Electrochem. Commun. 6 (2004) 71–74.
[28] Y. Saito, T. Kitamura, Y. Wada, S. Yanagida, Synth. Met. 131 (2002) 185–187.
[29] X.F. Lu, D.M. Chao, J.N. Zheng, J.Y. Chen, W.J. Zhang, Y. Wei, Polym. Int. 55 (2006) 945–950.
[30] T.M. Wu, Y.W. Lin, C.S. Liao, Carbon 43 (2005) 734–737.
[31] H. Arami, M. Mazloumi, R. Khalifehzadeh, S.H. Emami, S.K. Sadrnezhaad, Mater. Lett. 61 (2007) 4412–4415.
[32] C.Y. Wang, V. Mottaghitalab, C.O. Too, G.M. Spinks, G.G. Wallace, J. Power Sources 163 (2007) 1105–1109.
[33] D.A. Corrigan, R.M. Bandert, J. Electrochem. Soc. 136 (1989) 723–726.
[34] E. Laviron, J. Electroanal. Chem. 101 (1979) 19–28.
[35] K.N. Kuo, R.W. Marray, J. Electroanal. Chem. 131 (1982) 37–60.
[36] T. Komura, Y. Funahasi, T. Yamaguti, K. Takahasi, J. Electroanal. Chem. 446 (1998) 113–123.
[37] D.G. Christian, M.S. Adam, P.S. Greg, K. Janusz, M.T. Laren, J.Z. Zhang, Synth. Met. 132 (2003) 197–204.
[38] X.F. Lu, J.N. Zheng, D.M. Chao, J.Y. Chen, W.J. Zhang, Y. Wei, J. Appl. Polym. Sci. 100 (2006) 2356–2361.
[39] J. Wagner, J. Pielichowski, A. Hinsch, K. Pielichowski, D. Bogdał, M. Pajda, S.S. Kurek, A. Burczyk, Synth. Met. 146 (2004) 159–165.